Reply to: Rainfall an unlikely factor in Kīlauea's 2018 rift eruption

https://doi.org/10.1038/s41586-021-04164-0

Published online: 2 February 2022

Check for updates

Jamie I. Farquharson[1]✉ & Falk Amelung[1]

REPLYING TO M. P. Poland et al. *Nature* https://doi.org/10.1038/s41586-020-2172-5 (2022)

In the accompanying Comment[1], Poland et al. use rain gauge data to argue that, in contrast to the conclusion in our previously published paper[2], rainfall in the months leading up to the eruption was not anomalously high and that the eruption occurred in response to substantial magma pressurization. We demonstrate below that rain gauge data do in fact show anomalously high precipitation. Poland et al. miss this signal by looking only at the gauges furthest from the rift and by not accounting for the underlying distribution of the data. While we agree that there was precursory summit displacement (as we state in our Author Correction[3]) that prompted the U.S. Geological Survey to issue a Volcanic Activity Notice on 17 April, this does not necessarily suggest wholesale pressurization of the volcanic system. We show below that summit displacement was much less than before previous intrusions. Pressurization—however defined—does not preclude an external eruption trigger: eruptions are referred to as triggered[4–7] if they are precipitated by an external force regardless of whether pre-eruptive magma pressurization is evident[8].

Poland et al. claim that "no anomalous rainfall" is observed in nearby gauge data. There are five gauge locations in the vicinity of the rift zone at which data are available for the 2018 period (Fig. 1a). Of these, Poland et al. show data from those furthest from the rift—Hilo (repeated here: Fig. 1b, c) and two gauges near Kea'au—highlighting ten historical incidences of heightened rainfall recorded at each. However, they demonstrate no assessment of the underlying distribution of the time-averaged time series data, and provide no description of how they quantify 'anomalous' rainfall.

Closer to the rift, we observe the maximum recorded (data go back to 2009) daily values for two gauges in the Pahoa area (US1HIHI0051 and US1HIHI0003: Fig. 1a; the latter is shown in Fig. 1d, e). While we show here only gauges that cover the early 2018 period and for which super-decadal data are available, we note that 30-, 90- or 180-day maxima were also recorded by gauges at Pahoa, Kurtistown and Mountain View in the weeks before the eruption.

Further, as demonstrated in Fig. 1c, e, the underlying distributions of time-averaged rainfall are clearly non-normal; indeed, they are characterized by a lognormal distribution, as expected (rainfall cannot be negative) and as accounted for in our original Article. Any statistical evaluation of anomalous rainfall must take this distribution into account[9]; simply highlighting individual wet periods is arbitrary and unscientific. When the lognormal distribution is accounted for, the 90-day averages from both of the gauge datasets referred to by Poland et al. (Hilo and Kea'au) exhibit a >1ς (1 standard deviation) deviation from the long-term mean before the eruption (for example, Fig. 1b for Hilo). Moreover, gauges such as those at Pahoa (Fig. 1d)—closer to the rift zone than the examples chosen by Poland et al. (Fig. 1a)—exhibit deviations of greater than 2ς from the mean in the weeks before the 2018 eruption.

Poland et al. also suggest that satellite data for a 27-km^2 pixel covering the summit are not representative of precipitation throughout the rift zone and that our calibration method may unduly influence data in that pixel. As described in our Article, the described calibration is an empirical factor—determined using the Hawai'i Volcanoes National Park gauge (Fig. 1a)—bringing the absolute values of recorded rainfall in line with gauge data. By definition, this does not affect relative changes within the time series and so remains unaffected by the underestimation of rainfall in coastal areas by the Tropical Rainfall Measuring Mission (TRMM)[10]. Moreover, uncalibrated data for the adjacent pixels also show statistically anomalous rainfall (>1 or 2ς above the mean) before the eruption (Fig. 1g–k), including pixels mostly over the ocean. Thus, statistically anomalous rainfall is observed in independent gauge and satellite data (including datasets referred to by Poland et al.). This is especially pronounced for gauge data in the immediate vicinity of the rift zone (compare Fig. 1b, c with Fig. 1d, e).

Poland et al. infer substantial pressurization of the magmatic system in the weeks before the intrusion from (i) 20 cm of displacement of a Global Positioning System (GPS) station in the Pu'u 'ō'ō area, (ii) precursory mid-rift baseline rate change, (iii) 3- to 4-cm precursory lengthening of a summit caldera Global Positioning System baseline and (iv) lava lake level increase. The implication is that magma pressure increase reflects stress increase throughout the volcanic edifice.

(i) Around Pu'u'ō'ō, neither the magnitude nor the direction of displacement of GPS station PUOC is echoed in neighbouring stations (Fig. 2b, e, i), a fact that is misleadingly not reflected in Fig. 1a of ref. [1]. This station—approximately 25 m from the crater's edge—indicates shallow, highly localized changes in the system, and is clearly not representative of system deformation more broadly (for example, Fig. 2e). In fact, interferometric synthetic aperture radar (InSAR) observations show that the Pu'u'ō'ō area subsided (Fig. 2b, g). (ii) A detailed depiction of precursory mid-rift baseline change shows that the rate was not appreciably different to those of previous years and that there was little if any acceleration (Fig. 2m, n), in contrast to the interpolated signal of ref. [1] (their Fig. 1b). (iii) Although the horizontal GPS displacements around the northern caldera are generally consistent with the inflation of an intra-caldera source, the InSAR-observed subsidence (Fig. 2a) is not: the intrusion was precursed by transient deflation (possibly part of a deflation–inflation event) associated with subtle radial contraction and subsidence (Fig. 2h, i). This is in contrast to the situation in 2011, when InSAR data show the inflation signal above the Halema'uma'u chamber (Fig. 2c)[11]. A more detailed comparison with previous intrusions shows that the 2018 pre-intrusion vertical and baseline displacements were 1.7–3 times lower than in 2007 and 2011 (Fig. 2l, m). Indeed, the KTPM–NUPM baseline change in the lead-up to the 2018 eruption falls inside the range of secular change recorded in the same time period in previous years (2010, 2012–2017; Fig. 2n).

[1]Rosenstiel School of Marine and Atmospheric Science, University of Miami, Miami, FL, USA. ✉e-mail: jifarq89@googlemail.com

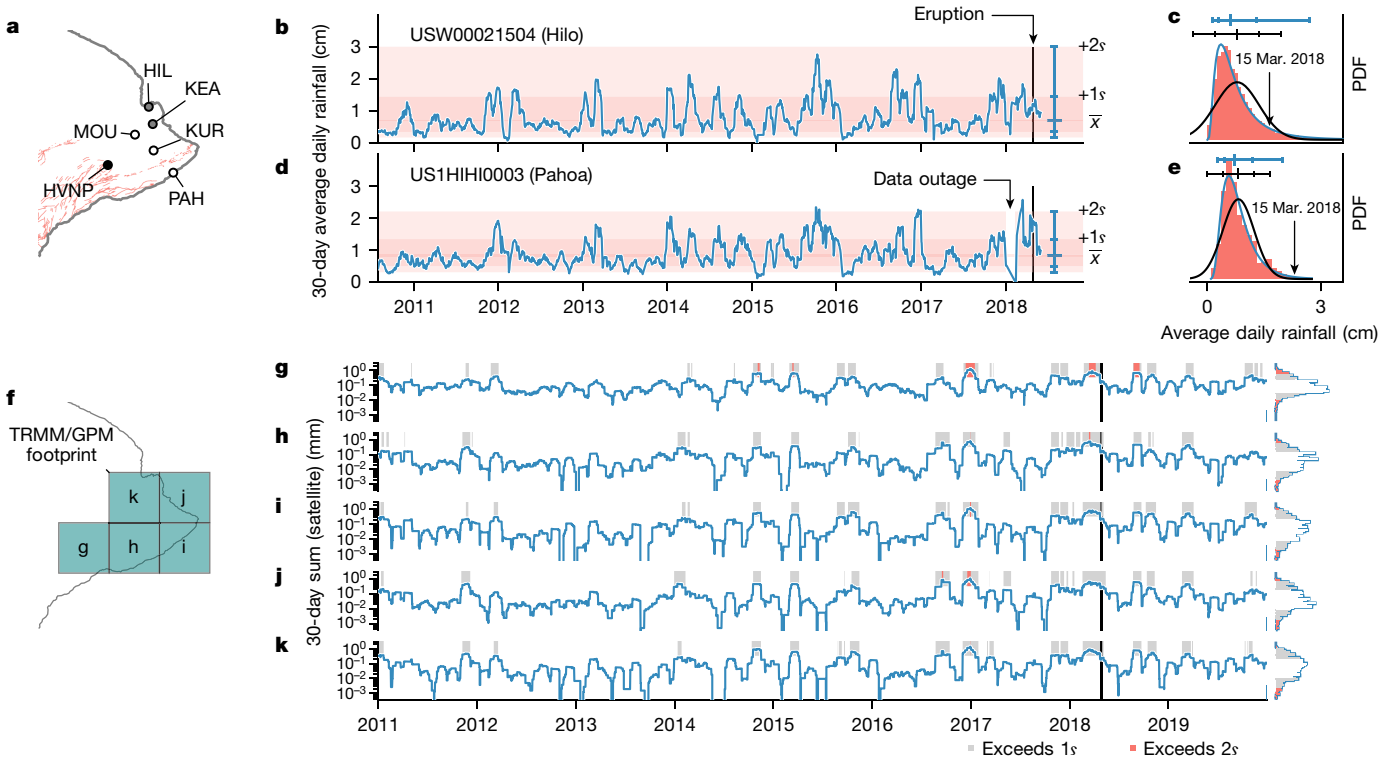

Fig. 1 | Pre-eruptive rainfall data. a, Location map showing gauges in the vicinity of the rift zone (fault system shown in red). HIL, Hilo International Airport (gauge USW00021504); KEA, Kea'au (USC00517023, USC00513872); KUR, Kurtistown (US1HIHI0055); MOU, Mountain View (US1HIHI0060, USC00516552); PAH, Pahoa (US1HIHI0008, US1HIHI0051, US1HIHI0003, USC00517457); HVNP, Hawai'i Volcanoes National Park (USC00511303). **b**, Thirty-day running average time series of Hilo gauge data. Solid vertical line indicates 2018 intrusion date. Mean ($\bar{x}$) and standard deviations (+1ς, +2ς) are highlighted, based on lognormal relationship shown in **c**. **c**, Probability density function (PDF) of Hilo gauge data from 1 Oct 1949 until 1 June 2018. Solid black and blue curves are best-fit normal and lognormal functions, respectively. Ticked black and blue lines at top of panel highlight −2ς, −1ς, $\bar{x}$, +1ς and +2ς distribution for either function. The 30-day average value two weeks before eruption is highlighted with an arrow. **d**, As **b**, for Pahoa gauge US1HIHI0003. **e**, As **c**, for Pahoa gauge between 1 July 2009 and 1 June 2018. **f**, Location map showing the footprints of five satellite data grids. **g**–**k**, Uncalibrated 30-day totals for different TRMM/Global Precipitation Measurement Mission (GPM) grid cells (**f**). For each time series, periods in which the windowed data exceed 1 and 2 standard deviations above the mean are highlighted. Marginal plots show histograms of windowed rainfall data, demonstrating the underlying lognormal distribution from which standard deviations are obtained (data from 2000 to 2020). Note that in early 2018, the rainfall signal is in all cases significantly greater than the mean at either the 1 or 2ς level.

(iv) Furthermore, the lava lake level increase before the 2018 intrusion of 20–30 m is substantially smaller than the ~100-m increase before the 2011 intrusion (associated with the same 'flow constriction' mechanism[12] posited here by Poland et al.) or even the ~50-m increase of large deflation–inflation events[13].

On the basis of recorded GPS displacements, Poland et al.[1] argue that there was substantial widespread pressurization before the 2018 intrusion. However, when viewed in the context of InSAR and geodetic data associated with both previous intrusions and periods of quiescence, the observed 2018 ground deformation was slight, altogether painting a picture of subtle and localized pressurization with a relatively minor effect on the volcanic edifice as a whole, particularly in the area where the 2018 intrusion initiated. Limited pressurization is characteristic of an 'open' magmatic system by definition. Nevertheless, we agree that the lake level increase indicates magma pressure increase and that it probably contributed to reaching the failure stress for dyke injection, while acknowledging that the relation between head change, magma pressure change and stress transfer into the edifice is complex owing to factors such as stratification and the presence of voids[11,14]. However, the effect of any subtle pressure increase on the stress regime in the edifice was local, whereas the infiltrated precipitation affects the rock strength throughout the edifice. In contrast to the situation in the early 2018 period, the inflation of the much larger south caldera reservoir to June 2017 resulted in 45-cm inflation and stress changes within a larger portion of the edifice. The difference in stress state between 2011 and 2018 highlighted by Poland et al. could reasonably be explained by inflation over this 2015–2017 period, along with ongoing progressive weakening of the edifice[15].

Choosing a different seasonal threshold, Poland et al. refute any significant long-term correlation between rain and eruptions at Kīlauea. Poland et al. assert that the correct threshold should be November–April, based on ref. [16], a point with which we disagree. Their argument does not accurately represent the previous work[16]: seasons proposed by ref. [16] are defined a priori and comprise an average for the entire state of Hawai'i. Moreover, those authors explicitly emphasize that 'windward areas' are an exception to the general annual rainfall cycle, indicating that the rift zone is not described by a November–April rainy season. In assuming this six-month season, the approach of Poland et al., to use their own words, "does not account for the complex patterns of rainfall and eruptions at Kīlauea"[1]. Our Fourier-based approach separates the periods of highest and least rainfall localized to the region of interest, which we deem preferable to a state-wide average known not to represent the rift zone.

We have not attempted to capture the complexity associated with defining the onset of previous eruptions (for example, "...several dyke intrusions"), instead using the published start dates from the Smithsonian Institution[17], which do not necessarily include precursory non-eruptive volcanic activity. This does not detract from the observation that intrusions into the rift zone appear to be approximately twice as likely to occur when subsurface pressure perturbations are

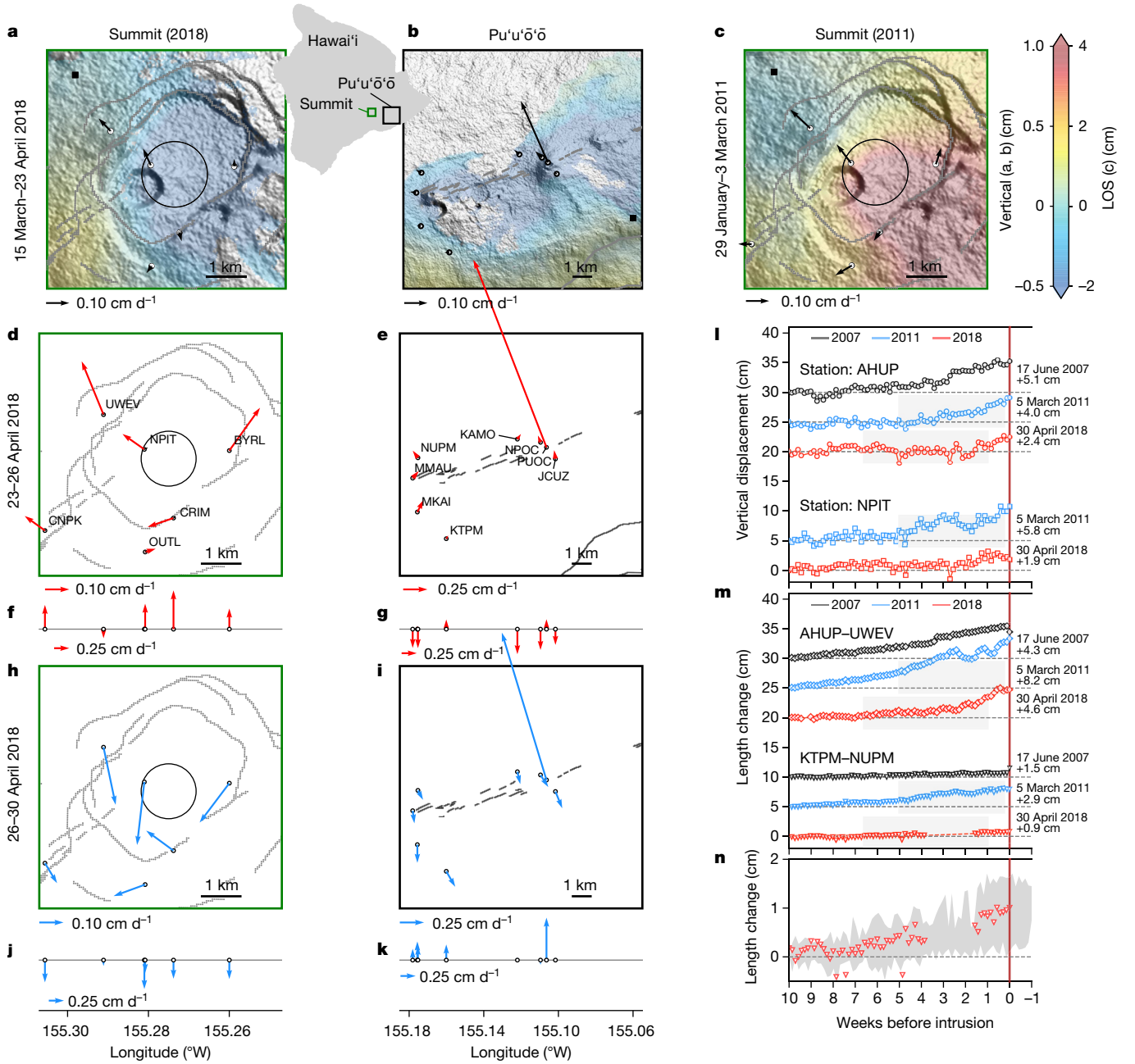

Fig. 2 | Precursory ground deformation at Kīlauea. a, **b**, Vertical displacement determined from Sentinel-1 InSAR data (ascending track 124 and descending track 87) for ~15 March 2018 to ~23 April 2018 (ascending: 15 March to 20 April 2018; descending: 18 March to 23 April 2018) at Kīlauea's summit (**a**), and the Pu'u'ō'ō region (**b**), together with horizontal GPS displacement vectors. Circle shows the estimated centroid location of the Halema'uma'u magma source. Black square is reference pixel. **c**, Line-of-sight (LOS) displacement (Cosmo-Skymed descending track 165) between 29 January and 2 March 2011. **d**, Horizontal GPS displacement between 23 April and 26 April at the summit. **e**, As **d**, for the Pu'u 'ō'ō region. **f**, Vertical GPS displacement at the summit between 23 and 26 April. **g**, As **f**, for Pu'u'ō'ō. **h**, Horizontal GPS displacement between 26 and 30 April at the summit. **i**, As **h**, for Pu'u'ō'ō. **j**, Vertical GPS displacement at the summit between 26 and 30 April. **k**, As **j**, for Pu'u'ō'ō. **l**, GPS time series for stations AHUP and NPIT, showing the vertical displacement before intrusions in 2007, 2011 and 2018. Solid vertical line represents intrusion. Annotations indicate intrusion dates and net displacement over the 10 weeks before. **m**, Line-length change between stations AHUP and UWEV (summit) and KTPM and NUPM (mid-rift), showing extensive displacement before intrusions in 2007, 2011 and 2018. **n**, Detailed view of length change between KTPM and NUPM stations. Red triangles show 2018 data and grey shaded region shows the range of evolution over the same months in previous years (2010, 2012–2017). Data for CNPK unavailable for time period in **a**. In **l**, **m**, time series data are offset from the *x*-axis for clarity, the shaded area indicates the corresponding InSAR epoch, and annotations indicate intrusion dates and net displacement over the 10 weeks before.

elevated above the running mean. Note that a significant correlation between rainfall and eruptions was reported in a previous U.S. Geological Survey study[18], although dismissed at the time because it was "difficult to imagine a physical triggering mechanism of rainfall on eruptions".

Poland et al. question the magnitude of computed rainfall-induced stress changes, suggesting that edifice fluid will be supercritical (thus, compressible) and that our permeability values are inappropriate. They also state that tide-induced pressure changes are greater than rainfall-induced perturbations.

While our stress changes are indeed small, this is probably often the case for eruption trigger stresses[19]; stress changes of 0.1–1 kPa are sufficient to induce failure in pre-stressed geological materials[20]. Temperatures for supercriticality are maintained only in the immediate vicinity of a magma body[21], whereas the mechanical influence of pore fluid can extend throughout the edifice. Our shallow permeability values are in line with recent studies of Kīlauea[22].

Theoretical tidal displacements at Kīlauea between April and June 2018 could effect positive pore pressure changes of at most around 0.1 kPa assuming realistic (poro-)elastic parameters (for example, elastic moduli[23]; Biot coefficient[24]). Moreover, Poland et al. draw a false equivalence here: stress perturbations required for mechanical failure by (high-frequency, short-period) dynamic stressors are higher than those required for static or quasi-static stresses[25], as we state in our Article.

As a final note, we highlight that Poland et al. refer to four articles that were unpublished and thus unavailable at the time of writing; indeed, one of these is a solicited News & Views piece that accompanied our original Article.

Data availability

All data are open source. Satellite-derived rainfall data (TRMM and GPM satellite data) are available from the NASA (National Aeronautics and Space Administration) EarthData Goddard Earth Sciences Data and Information Services Center portal (https://doi.org/10.5067/TRMM/TMPA/3H/7). Rainfall gauge data are available from the National Oceanic and Atmospheric Administration's National Centers for Environmental Information climate data portal (https://www.ncdc.noaa.gov/cdo-web/datasets/GHCND/stations/GHCND:USC00511303/detail). GPS data are available from the Nevada Geodetic Laboratory (http://geodesy.unr.edu/NGLStationPages/stations/). Sentinel-1 ascending- and descending-track SAR acquisitions were obtained through UNAVCO's Seamless SAR Archive (https://doi.org/10.5194/isprsarchives-XL-1-65-2014). Derived time series products of Kīlauea are available at https://doi.org/10.5281/zenodo.3944709 and https://doi.org/10.5281/zenodo.3957859.

Code availability

Code required for data access, analysis and display is available, in Jupyter Notebook format, at https://github.com/jifarquharson/Farquharson_Amelung_2020_Kilauea-Nature/blob/master/Farquharson_Amelung_Kilauea_Supplemental_2.ipynb (Fig. 1) and https://github.com/jifarquharson/Farquharson_Amelung_2020_Kilauea-Nature/blob/master/Farquharson_Amelung_Kilauea_Supplemental_1.ipynb (Fig. 2).

1. Poland, M. P. et al. Rainfall an unlikely factor in Kīlauea's 2018 rift eruption. *Nature* https://doi.org/10.1038/s41586-020-2172-5 (2022).
2. Farquharson, J. I. & Amelung, F. Extreme rainfall triggered the 2018 rift eruption at Kīlauea Volcano. *Nature* **580**, 491–495 (2020).
3. Farquharson, J. I. & Amelung, F. Author Correction: Extreme rainfall triggered the 2018 rift eruption at Kīlauea Volcano. *Nature* **582**, E3 (2020).
4. Dzurisin, D. Influence of fortnightly earth tides at Kilauea Volcano, Hawaii. *Geophys. Res. Lett.* **7**, 925–928 (1980).
5. Lipman, P. W., Lockwood, J. P., Okamura, R. T., Swanson, D. A. & Yamashita, K. M. *Ground Deformation Associated with the 1975 Magnitude-7.2 Earthquake and Resulting Changes in Activity of Kilauea Volcano, Hawaii* (1985).
6. Poland, M. P., Sutton, A. J. & Gerlach, T. M. Magma degassing triggered by static decompression at Kīlauea Volcano, Hawai'i. *Geophys. Res. Lett.* **36**, L16306 (2009).
7. Orr, T. R., Thelen, W. A., Patrick, M. R., Swanson, D. A. & Wilson, D. C. Explosive eruptions triggered by rockfalls at Kīlauea volcano, Hawai'i. *Geology* **41**, 207–210 (2013).
8. *Volcano Hazards Program FAQs* (USGS, 2011); https://volcanoes.usgs.gov/vsc/file_mngr/file-153/FAQs.pdf
9. Oosterbaan, R. J. in **Vol. 16** 175–224 (IILRI, 1994).
10. Chen, Y., Ebert, E. E., Walsh, K. J. E. & Davidson, N. E. Evaluation of TRMM 3B42 precipitation estimates of tropical cyclone rainfall using PACRAIN data. *J. Geophys. Res. Atmos.* **118**, 2184–2196 (2013).
11. Bagnardi, M. et al. Gravity changes and deformation at Kīlauea Volcano, Hawaii, associated with summit eruptive activity, 2009–2012. *J. Geophys. Res. Solid Earth* **119**, 7288–7305 (2014).
12. Patrick, M. R., Anderson, K. R., Poland, M. P., Orr, T. R. & Swanson, D. A. Lava lake level as a gauge of magma reservoir pressure and eruptive hazard. *Geology* **43**, 831–834 (2015).
13. Anderson, K. R., Poland, M. P., Johnson, J. H. & Miklius, A. in *Hawaiian Volcanoes* 229–250 (American Geophysical Union, 2015).
14. Parfitt, L. & Wilson, L. *Fundamentals of Physical Volcanology* (Wiley, 2009).
15. Wauthier, C., Roman, D. C. & Poland, M. P. Modulation of seismic activity in Kīlauea's upper East Rift Zone (Hawai'i) by summit pressurization. *Geology* **47**, 820–824 (2019).
16. Frazier, A. G. & Giambelluca, T. W. Spatial trend analysis of Hawaiian rainfall from 1920 to 2012. *Int. J. Climatol.* **37**, 2522–2531 (2017).
17. *Global Volcanism Program, 2013. Volcanoes of the World* Version 4.9.1 (accessed 17 September 2020); https://doi.org/10.5479/si.GVP.VOTW4-2013.
18. Klein, F. W. Eruption forecasting at Kilauea Volcano, Hawaii. *J. Geophys. Res. Solid Earth* **89**, 3059–3073 (1984).
19. Díez, M., Femina, P. C. L., Connor, C. B., Strauch, W. & Tenorio, V. Evidence for static stress changes triggering the 1999 eruption of Cerro Negro Volcano, Nicaragua and regional aftershock sequences. *Geophys. Res. Lett.* **32**, L04309 (2005).
20. Hainzl, S., Kraft, T., Wassermann, J., Igel, H. & Schmedes, E. Evidence for rainfall-triggered earthquake activity. *Geophys. Res. Lett.* **33**, L19303 (2006).
21. Hayba, D. O. & Ingebritsen, S. E. Multiphase groundwater flow near cooling plutons. *J. Geophys. Res. Solid Earth* **102**, 12235–12252 (1997).
22. Hsieh, P. A. & Ingebritsen, S. E. Groundwater inflow toward a preheated volcanic conduit: application to the 2018 eruption at Kīlauea Volcano, Hawai'i. *J. Geophys. Res. Solid Earth* **124**, 1498–1506 (2019).
23. Heap, M. J. et al. Towards more realistic values of elastic moduli for volcano modelling. *J. Volcanol. Geotherm. Res.* **390**, 106684 (2020).
24. Farquharson, J., Heap, M. J., Baud, P., Reuschlé, T. & Varley, N. R. Pore pressure embrittlement in a volcanic edifice. *Bull. Volcanol.* **78**, 6 (2016).
25. Li, D., Wang, T., Cheng, T. & Sun, X. Static and dynamic tensile failure characteristics of rock based on splitting test of circular ring. *Trans. Nonferrous Met. Soc. China* **26**, 1912–1918 (2016).

Acknowledgements Copernicus Sentinel-1 and Cosmo-Skymed SAR data are available thanks to the Group on Earth Observation's Geohazard Supersites and Natural Laboratory Initiative. This work was supported by funding from NASA's Interdisciplinary Research in Earth Science programme (grant number 80NSSC17K0028 P00003). Data processing was conducted using Stampede2 at the Texas Advanced Computing Center of the Extreme Science and Engineering Discovery Environment, supported by National Science Foundation grant number ACI-1548562, using the public domain InSAR Scientific Computing Environment software of the Jet Propulsion Laboratory. We thank B. Varugu for discussions.

Author contributions J.I.F. processed the GPS and rainfall data, and plotted all data. F.A. processed the InSAR data. Both authors contributed to the writing.

Competing interests This work was supported by funding from NASA's Interdisciplinary Research in Earth Science programme (grant number 80NSSC17K0028 P00003) exploring the influence of rainfall in triggering volcanism.

Additional information
Correspondence and requests for materials should be addressed to Jamie I. Farquharson.